Hindawi Publishing Corporation
Advances in Optical Technologies
Volume 2008, Article ID 295601, 10 pages
doi:10.1155/2008/295601

Research Article

Light Emission from Rare-Earth Doped Silicon Nanostructures

J. Li, O. H. Y. Zalloum, T. Roschuk, C. L. Heng, J. Wojcik, and P. Mascher

Department of Engineering Physics and Centre for Emerging Device Technologies, McMaster University, Hamilton, ON, Canada L8S 4K1

Correspondence should be addressed to P. Mascher, mascher@mcmaster.ca

Received 5 December 2007; Accepted 27 March 2008

Recommended by D. Lockwood

Rare earth (Tb or Ce)-doped silicon oxides were deposited by electron cyclotron resonance plasma-enhanced chemical vapour deposition (ECR-PECVD). Silicon nanocrystals (Si-ncs) were formed in the silicon-rich films during certain annealing processes. Photoluminescence (PL) properties of the films were found to be highly dependent on the deposition parameters and annealing conditions. We propose that the presence of a novel sensitizer in the Tb-doped oxygen-rich films is responsible for the indirect excitation of the Tb emission, while in the Tb-doped silicon-rich films the Tb emission is excited by the Si-ncs through an exciton-mediated energy transfer. In the Ce-doped oxygen-rich films, an abrupt increase of the Ce emission intensity was observed after annealing at 1200°C. This effect is tentatively attributed to the formation of Ce silicate. In the Ce-doped silicon-rich films, the Ce emission was absent at annealing temperatures lower than 1100°C due to the strong absorption of Si-ncs. Optimal film compositions and annealing conditions for maximizing the PL intensities of the rare earths in the films have been determined. The light emissions from these films were very bright and can be easily observed even under room lighting conditions.

Copyright © 2008 J. Li et al. This is an open access article distributed under the Creative Commons Attribution License, which permits unrestricted use, distribution, and reproduction in any medium, provided the original work is properly cited.

1. INTRODUCTION

The realization of integrated silicon photonics requires the development of several fundamental components including light sources, modulators, amplifiers, and detectors [1, 2]. To achieve silicon-based light sources has always been the most challenging task, with the first optically pumped silicon Raman laser being reported only very recently [3]. It is well known that bulk silicon is a poor light emitter due to its indirect bandgap and the presence of nonradiative recombination pathways [4]. Many approaches have been attempted to overcome these obstacles and achieve efficient emission from silicon. One of the most promising solutions is to introduce impurities such as rare-earth elements into materials. Of the rare-earth elements, Er has attracted the most extensive attention because of the coincidence between its intra-4f transition at 1535 nm and the transparency window used for telecommunications [5]. However, the demand to realize full-color light emission from silicon structures can extend technology interests to many other rare-earth elements such as Tb and Ce which usually emit green and ultraviolet/blue light, respectively [6].

Luminescence from rare-earths has been studied extensively since it was discovered at the beginning of the 20th century [7]. Today various rare-earth doped materials are playing important roles in many areas such as displays, solid-state lasers, detectors, and data storage [8–12]. Recently, there have arisen enormous demands to develop optical sources and amplifiers compatible with silicon ULSI technology leading to a large increase in the interest for one specific type of material: rare-earth doped silicon-based materials [6].

Rare-earth elements make up the sixth row of the periodic table and have a partially filled 4f shell. Optically active rare-earth ions often exist as trivalent and are formed by losing one 4f electron and both 6s electrons. Luminescence from these ions is mainly attributed to their intra-4f or 5d-4f transitions. Intra-4f transitions are relatively independent of the host material, since the 4f states are shielded from outside interaction by 5d states. Note that intra-4f transitions for free ions are parity forbidden but are partially allowed

through the mixing of opposite parity wave functions when rare-earth ions are embedded in a host material. As a result, they have very long luminescence lifetimes and weak oscillator strengths. In contrast, 5d-4f transitions are very sensitive to the surrounding ligands because 5d states are directly exposed to the local environment. Thus, changes in the spectral shapes, peak positions, and intensities may suggest the evolution of the matrix structure. Additionally, since 5d-4f transitions are parity permitted, they have very short luminescence lifetimes and strong oscillator strengths [13].

There are two major obstacles that have to be overcome in order to achieve efficient emission from rare-earth doped silicon oxides: inefficient excitation of intra-4f transitions from rare-earth ions and low solubility of optically active rare-earth ions in silicon-based hosts.

Emissions from rare-earth ions often originate from the intra-4f transitions which are only partially parity allowed. As a result, many rare-earth ions suffer from constraints on excitation wavelengths and their low absorption cross-sections of pump photons. For example, Er ions embedded in silica can only be directly excited at several specific wavelengths including 488, 514, 800, 980, and 1480 nm and the absorption cross-section is as low as 10^{-21} to 10^{-20} cm^2 [5]. Various sensitizers such as Yb ions, silicon nanocrystals (Si-ncs), silver, and organic complexes have been found to be able to enhance rare-earth emission significantly through a dipole-dipole Forster-Dexter coupling process [14].

One structure receiving particular attention is Er-doped silicon-rich silicon oxide (SRSO). The Si-ncs precipitated upon annealing can be considered as three-dimensionally confined structures. The "bandgap" (energy difference between the highest occupied molecularorbital (HOMO) and the lowest unoccupied molecular orbital (LUMO)) of these structures increases with a decrease in size due to quantum confinement effects [15]. It was demonstrated that Er emission can be enhanced significantly through exciton-mediated energy transfer between Si-ncs and Er [16].

Great efforts have been made to understand the physics of the Er:Si-ncs system. The sensitization mechanism is now relatively well understood at the phenomenological level. After a Si-nc absorbs a photon, a bound exciton is generated in the Si-nc. The exciton may recombine nonradiatively by transferring energy to a nearby Er ion, putting the ion into an excited state. The Er ion then decays to the ground stateby emitting a photon of 1.54 μm [14]. According to the generalized rate-equation analysis by Kenyon et al. [17], this sensitization process is strongly dependent on the distance between the Si-nc and Er ion. The Er luminescence is thus limited by the low number of Er ions coupled to the Si-ncs, which is due to the low Si-ncs density and the short interaction distance.

Since Si-ncs have a high absorption cross-section and efficiently transfer energy to Er ions, the excitation cross-section of Er ions can be increased by up to 10^4 times [16]. Furthermore, the absorption band of Si-ncs covers the whole visible spectrum and the utilization of broad band excitation sources becomes possible. The successful excitation of Er in SRSO using a broad band visible excitation source, such as a commercial camera flashgun or blue LED has been demonstrated [18, 19].

In principle, an analogous excitation mechanism can operate in SRSO films doped with other rare-earths as long as the "bandgap" of Si-ncs wide enough to ensure energy transfer to the rare-earth ions [20]. In the present work, we demonstrate that by using a 325 nm He-Cd laser the Tb emission can be excited efficiently in both SRSO and oxygen-rich silicon oxides (ORSO) through different excitation processes.

The solubility of optically active rare-earth ions in various silicon materials is universally low due to the mismatch of ionic radii and the strong covalent bonding of the matrix network. Above the critical concentrations, rare-earth ions tend to form precipitates, which results in severe luminescence quenching through ion-ion interaction or by forming an optically inactive phase [6]. It is very difficult to incorporate high concentrations of optically active rare-earths in silicon materials through equilibrium techniques such as the sol-gel method [21]. Low temperature techniques, such as ion implantation or plasma enhanced chemical vapor deposition (PECVD), are able to increase the solubility limit by an order of magnitude, an effect attributed to the lower diffusivity of the dopant ions. Particularly, electron cyclotron resonance (ECR)-PECVD can generate a uniform distribution of rare-earth doping throughout the entire film thickness with low defect concentrations due to the low ion energy [22].

Over the past few years, we have been conducting extensive studies on achieving highly efficient light emission from rare-earth doped silicon nanostructures formed in thin films prepared by ECR-PECVD. It was found that Er emission properties are highly dependent on the details of Si-ncs and Er concentrations. The Er emission intensities can be enhanced greatly by optimizing deposition parameters and postdeposition thermal annealing conditions [23, 24].

In this paper, we report on studies of SRSO and ORSO doped with Tb or Ce. We show successful in situ incorporation of high concentrations of rare-earth elements. The dependence of the emission properties on rare-earth dopant concentration, silicon/oxygen ratio, and annealing temperature was investigated. The emission intensities from the rare-earths were optimized. An interpretation of the excitation mechanisms and the correlation between optical properties and structural evolution is suggested.

2. EXPERIMENTAL DETAILS

Tb or Ce doped silicon oxides were prepared in a custom-designed ECR-PECVD system (**Figure 1**). Ar and O_2 plasma gases were introduced from the upper dispersion ring. Silane (SiH_4) gas diluted in Ar was used as the Si source and volatile metal-organic precursors served as the rare-earth sources. $Tb(tmhd)_3$ or *tris (2,2,6,6-teramethyl-3,5-heptanedionato)-Tb(III)*, and $Ce(tmhd)_3$ or *tris (2,2,6,6-teramethyl-3,5-heptanedionato)-Ce(III)*) were used as the Tb and Ce sources, respectively. The rare-earth sources were contained in a manifold which can be heated up to 200°C to sublime the precursor inside. Ar carrier gas then transports

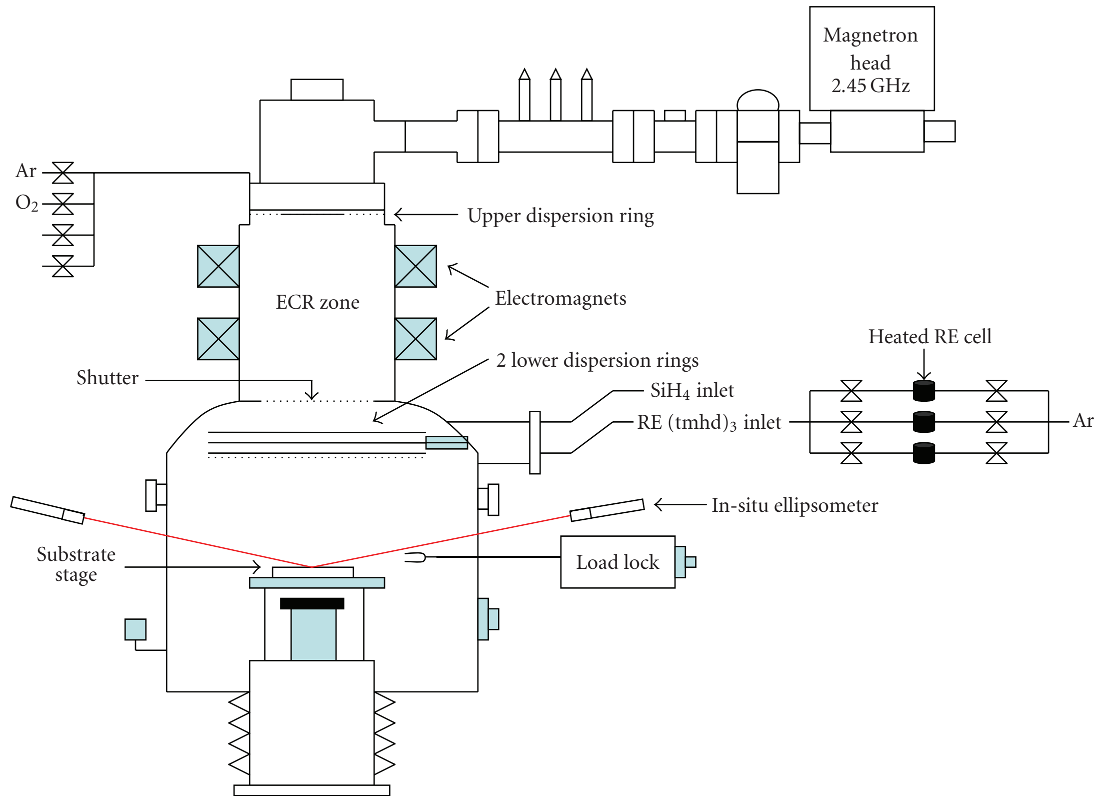

Figure 1: ECR-PECVD system.

the rare-earth precursor through a transmission line after which it is introduced in the chamber alongside the SiH_4 through the lower dispersion ring. This multidopant delivery system allows the incorporation of up to three types of rare-earth elements simultaneously. The temperatures of three rare-earth manifold containers, the rare-earth dispersion ring, and the transmission lines are independently controlled by five Eurotherm temperature controllers. All of the gas flow rates can be controlled independently using a central mass flow controller panel. The base pressure of the system was 1×10^{-7} Torr and the deposition pressure was between 2 and 5 mTorr.

Rare-earth doped silicon oxide films were deposited on n-type (100) silicon wafers which sit on the substrate stage located in the reaction chamber. In the present study, the stage temperature was 350°C, but it could be varied from room temperature to 800°C. The film thickness was monitored during the deposition by an in situ ellipsometer operating at 632.8 nm. Several deposition parameters including rare-earth cell temperature, SiH_4 and O_2 gas flows, and microwave power were varied to achieve different Si, O, and rare-earth content. A summary of the deposition parameters and their values in this study are given in Table 1. Two types of mass flow controller were used for different samples, therefore, there are two types of flow rate units employed as indicated in Table 1. Each sample contains only one type of rare-earth dopant. The thicknesses of all the samples were remeasured after the deposition through ellipsometry and vary from 800–1100 Å. All PL intensities discussed in this report were normalized to 1000 Å, assuming that PL intensity increases linearly with thickness.

The compositions of the samples were determined quantitatively through Rutherford backscattering spectrometry (RBS) using a 1.0 MeV He^+ beam confirming the successful incorporation of rare-earth elements into the thin films. Figure 2 shows the RBS spectrum of an as-deposited Ce-doped sample containing 32 at.% Si and 1.0 at.% Ce. The energies related to the surface Ce, Ar, Si, and O atoms are as indicated. The signal from O sits on the signal from Si in the substrate and depresses the signal from Si in the film. Si, O, and Ce all exhibit a uniform concentration distribution throughout the film thickness. Trace amounts of Ar are also observed in the spectrum. The majority of Ar can be removed from the film during annealing. In the present study, the Si content varies from 32 to 40 at.%, Tb 0.1 to 0.8 at.%, and Ce 0.01 to 1.0 at.%.

All the films were annealed in a quartz tube furnace under flowing N_2 for 1 hour. The annealing temperature varied from 800 to 1200°C. The luminescence properties of the films were analyzed by single wavelength laser-excited PL spectroscopy. The excitation source was a 17 mW He-Cd laser operating at 325 nm. The PL from the films was detected by a spectrometer employing a charge-coupled device array; these PL spectra were corrected for system response and optics transmission and subsequently converted to normalized photon flux. A full description of the CCD-based

Table 1: Summary of the deposition parameters and their values for the depositions in this study.

Dopant type	RE concentration [at.%]	Si concentration [at.%]	Forwarded power [W]	Reflected power [W]	SiH_4 flow rate	O_2 flow rate	Ar flow rate	RE cell temp [°C]
Tb	0.4[(2)]	32	420	10	7	24	20	160
	0.8[(2)]	32	420	10	7	24	30	160
	0.1[(2)]	36	608	7	20	60	25	160
	0.2[(2)]	38	327	27	20	56	25	156
	0.3[(2)]	36	500	5	20	56	25	153
Ce	0.01[(2)]	33	510	5	11	78	12	100
	0.1[(3)]	32	507	7	4	40	25	180
	1.0[(3)]	32	509	7	2	30	10	200
	0.04[(2)]	40	515	5	25	70	12	161

(2) The sample was deposited using mass flow controller 1, the corresponding flow rate unit is mV.
(3) The sample was deposited using mass flow controller 2, the corresponding flow rate unit is sccm.

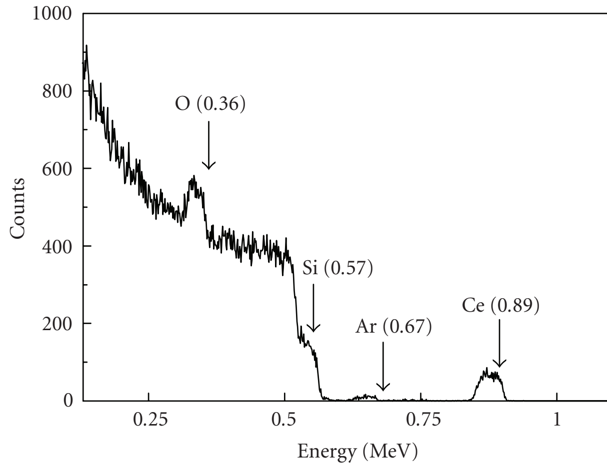

Figure 2: RBS measurement of a Ce:ORSO sample containing 32 at.% Si and 1.0 at.% Ce. The surface energies of Ce, Ar, Si, and O are indicated by arrows.

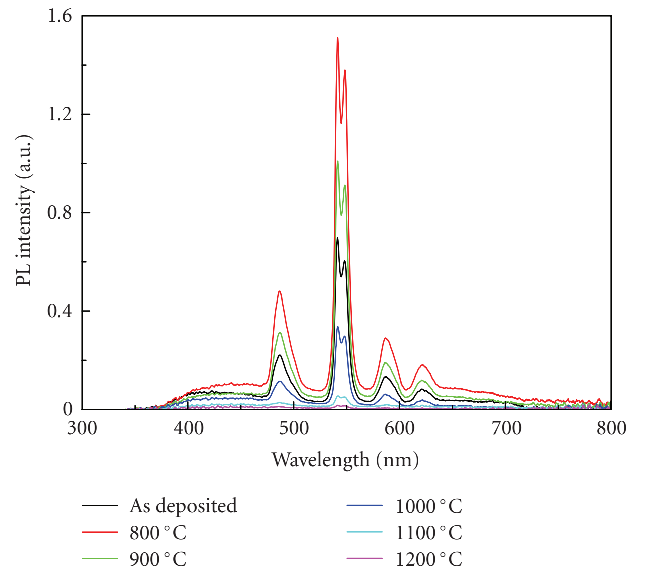

Figure 3: PL spectra of the Tb:ORSO samples containing 0.4 at.% Tb, as deposited and annealed at different temperatures in the range of 800–1200°C.

PL system and the data correction methodology is given elsewhere [25]. All the measurements were performed at room temperature. The formation of Si-ncs in the Tb doped silicon-rich film was studied by a JEOL 2010F Field Emission Gun Transmission Electron Microscope operating at 200 keV.

3. RESULTS AND DISCUSSION

3.1. Tb doped oxygen-rich silicon oxides (Tb:ORSO)

The Tb:ORSO samples have a constant Si content of 32 at.% and varying Tb content of 0.4 and 0.8 at.%, respectively. Figure 3 shows the PL spectra of the 0.4 at.% Tb sample as-deposited and annealed at various temperatures. Four strong distinct sharp bands were observed sitting on a weak broad band for all annealing temperatures. According to the energy level diagram of Tb^{3+} ions shown in Figure 4 [adapted from [26]], the four bands centered at 487, 546, 588, and 620 nm are related to $^5D_4 - {}^7F_j$ ($j = 6, 5, 4, 3$) intra-4f transitions of Tb^{3+}. The 546 nm band is split into two peaks, centered at 542 and 548 nm, due to the Stark splitting of the matrix. The emissions from the $^5D_3$ state are absent due to the cross-relaxation effect [27]. The observed emission spectra resemble those of Tb doped SiO_2 fabricated by conventional PECVD [28]. The peak around 546 nm has been confirmed to originate from Tb^{3+} using PL decay measurements [29]. The corresponding lifetime was around 1.3 ms. There are no appreciable changes in the peak positions and spectral widths with annealing temperature.

The weak broadband emission ranging from 400 to 700 nm is usually attributed to oxide defects in the matrix [30]. If that were indeed the case, the corresponding emission should decrease after annealing at 800°C, since the defects in SiO_2 tend to reduce during annealing process.

However, in this study the emission became stronger after annealing at 800°C. In addition, this unidentified emission and the Tb emission have a similar dependence on annealing temperature. Therefore, we suggest that the origin is related to the optically active Tb^{3+} sites.

It is important to note that the 325 nm (3.8 eV) excitation is not resonant with any optical absorption band of Tb^{3+}, so the observation of the strong Tb emission from the film implies the presence of a highly efficient indirect excitation process. In general, there are two types of indirect excitation mechanisms: carrier-mediated excitation and dipole-dipole Forster-Dexter coupling [6]. A previous investigation on Tb-doped silicon oxynitrides by Jeong et al. has suggested that Tb^{3+} ions can be excited efficiently by a 325 nm excitation source through carrier recombination processes [31]. The 325 nm source is able to excite carriers into extended above-band-gap states, because the bandgap of silicon oxynitride is only between 3.5 to 4 eV for the samples they considered [32]. However, for the films considered here, this process is less possible, because the bandgap of SiO_2 is as large as 8 eV. In oxygen-rich films, it is expected that no or very few Si-ncs exist. Based on this assumption, the presence of alternate sensitizers has to be considered.

One possible sensitizer is the organic molecule introduced during the deposition from the metal organic precursor $Tb(tmhd)_3$. It was found that some rare-earth chelates have broad absorption bands and high absorption coefficients and can serve as sensitizers to efficiently excite rare-earth ions. Many rare-earth chelates have been synthesised to exploit the effect [14]. To the best of our knowledge, however, there have been no reports on the sensitizing effect of the $Tb(tmhd)_3$ molecules employed in the present study. Further studies on the absorption properties of the sensitizer clearly are necessary.

Figure 5 shows the 546 nm peak intensities of various samples as a function of annealing temperature between 800 and 1200°C. The intensities generally decrease with an increase of the annealing temperature. In comparison to the as-deposited sample, the significant enhancement of the Tb emission after annealing at 800°C can be attributed to the reduction of defects and the activation of optically active Tb^{3+} sites. The decrease of the Tb emission at annealing temperatures higher than 800°C can be explained by the reduction of both optically active Tb sites and available sensitizers. X-ray absorption fine structure (XAFS) analysis has confirmed that there are two types of Tb sites existing in Tb-doped SiO_2:Tb coordinated with two oxygen atoms (Tb-2O) or six oxygen atoms (Tb-6O), with the formation of the latter being related to the enhancement of Tb emission [33]. At annealing temperatures higher than 800°C, Tb ions achieve enough energy to diffuse and form clusters. So the number of oxygen atoms associated with each Tb ion is reduced, which may lead to the transformation from Tb-6O to Tb-2O and results in the decrease of Tb emission. Another possibility that cannot be excluded is that the organic molecules become more unstable and begin to dissociate at higher annealing temperatures. As a result, the available sensitizers may reduce significantly and also lead to the decrease of Tb emission.

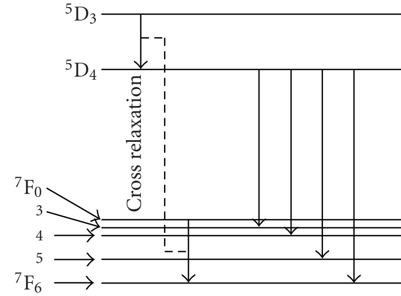

Figure 4: The electronic energy levels of Tb^{3+} [adapted from [26]].

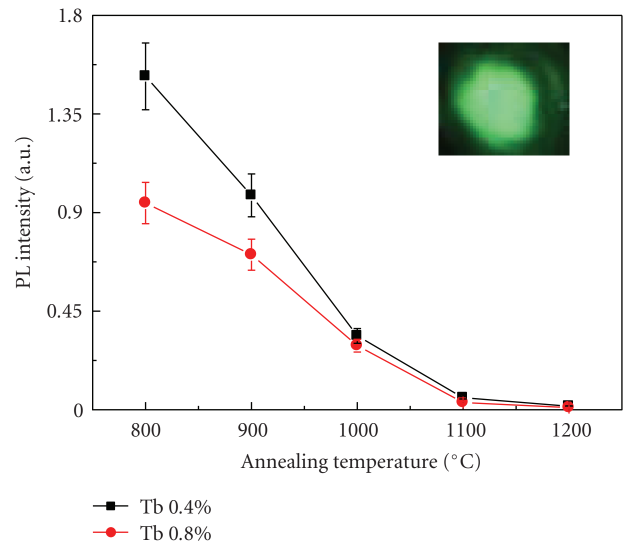

Figure 5: PL intensity of Tb^{3+} at 546 nm from two Tb:ORSO samples as a function of annealing temperature. The inset shows an image of strong green Tb emission from the 0.4 at.% Tb sample after annealing at 800°C taken by camera.

Since a previous study on Tb doped SiO_2 showed that the lifetime of Tb emission still remains almost constant at concentration as high as 2.7 at.% [29], our observation of the decrease of the emission intensity at high Tb concentration might not be due to ion-ion interaction and is possibly attributable to the trend to form clusters which leads to the reduction of optically active Tb-6O sites or the exhaustion of available sensitizers.

In this study, the strongest Tb emission was observed from the 0.4 at.% Tb sample annealed at 800°C. The inset of Figure 5 shows the corresponding picture taken with a camera. The emission was quite strong and can be easily observed under bright room lighting conditions.

3.2. *Tb-doped silicon-rich silicon oxide (Tb:SRSO)*

The Tb:SRSO samples have a constant Si content of 36 at.% and varying Tb content of 0.1, 0.2, and 0.3 at.%, respectively. Figure 6 shows the PL spectra of the 0.3 at.% Tb sample as-deposited and annealed at various temperatures. A broad emission band centered at 650 nm was observed from the

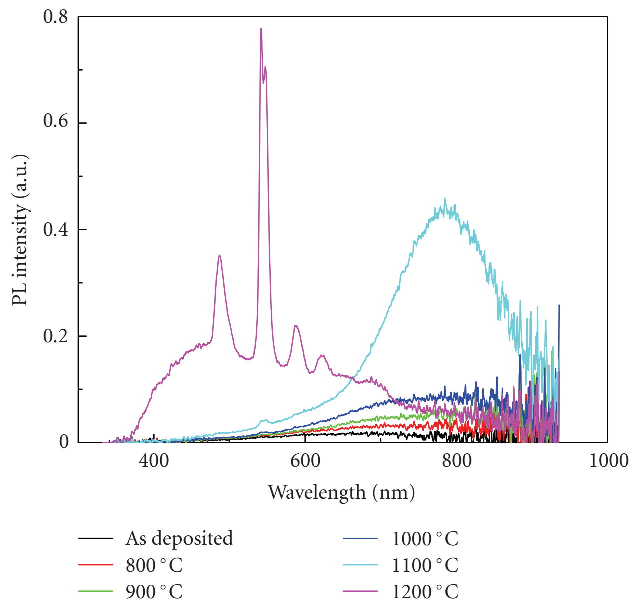

Figure 6: PL spectra of the Tb:SRSO samples containing 0.3 at.% Tb, as-deposited or annealed at various temperatures in the range of 800–1200°C.

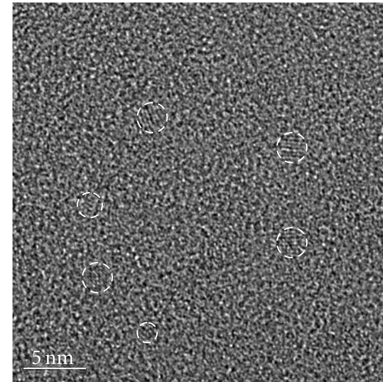

Figure 7: HR-TEM image of a Tb:SRSO sample containing 0.3 at.% Tb annealed at 1100°C.

as-deposited sample. Annealing at temperatures between 800 and 1100°C results in an increase in its intensity with a red shift of the peak position. This is characteristic of Si-ncs emission. The enhancement of the emission intensity indicates the formation of more Si-ncs, while the red shift of the peak suggests the growth of the Si-ncs sizes.

A weak emission band peaking at 546 nm emerged after annealing at 1100°C. After annealing at 1200°C, the Si-ncs emission decreases abruptly. At the same time, the four sharp peaks centered at 487, 546, 588, and 620 nm become dominant. Both the weak 546 nm peak observed after annealing at 1100°C and the four strong sharp peaks observed after annealing at 1200°C originate from intra-4f transitions of Tb^{3+} ions.

As mentioned in the previous section, the 325 nm excitation is not resonant with any absorption band of Tb^{3+} ions and the observation of Tb emission indicates the existence of (an) indirect excitation mechanism(s). The simultaneous quenching of the Si-ncs emission and the increase of the Tb emission intensity after annealing at 1200°C suggests the efficient energy transfer from Si-ncs to Tb^{3+} ions. Here, we attribute the observed Tb emission to the exciton energy transfer process. This mechanism may appear questionable, since the PL of Si-ncs after annealing at 1200°C is peaking around 800 nm (1.55 eV), while at least 2.5 eV (488 nm) energy is required to excite Tb^{3+}. However, it has been suggested that when the sizes of Si-ncs reduce to less than 3 nm, the infrared PL of Si-ncs is due to the recombination of the excitons trapped in oxygen-related localized states. Therefore, the actual "bandgap" of an Si-nc might be much higher than that indicated by its emission wavelength [15]. Figure 7 shows a high-resolution transmission electron microscopy (HR-TEM) image of a Tb:SRSO sample containing 0.3 at.% Tb annealed at 1100°C. The clear lattice fringes shown in the circle areas reveal the formation of Si-ncs. The sizes of Si-ncs are around 2 nm. The "bandgap" of a 2 nm Si-nc can be as high as 2.5 eV as a result of quantum confinement effects [15], which is sufficient for the excitation of Tb^{3+}.

Although the organic sensitizer-Tb $(tmhd)_3$ may also be present in the silicon-rich samples, the absence of the Tb emission from the samples as-deposited and after annealing between 800 and 1200°C indicates that the corresponding excitation is not very efficient. One possible explanation is that the Si-ncs are dominant in the absorption of excitation photons due to their relatively high absorption coefficient [6]. In particular, the organic sensitizers are less likely to be responsible for the strong Tb emission after annealing at 1200°C, since the Tb emission intensity of the silicon-rich sample containing 0.3 at.% Tb is 50 times higher than that of the oxygen-rich sample containing 0.4 at.% Tb after annealing at the same temperature.

Figure 8 shows the emission intensities of Si-ncs in the samples with various Tb concentrations as a function of annealing temperature. The Si-ncs emission was observed to decrease with the increase of Tb concentration at annealing temperatures greater than 900°C. Although Tb emission was only appreciable from the samples annealed at 1100 and 1200°C, this decrease is indicative that the energy transfer between Si-ncs and Tb^{3+} ions is also occurring at 1000°C, thereby suppressing the Si-ncs PL. The inset of Figure 8 shows that after annealing at 1200°C, the intensity of the Tb^{3+} 546 nm emission increases with the Tb concentration, which can be explained by an increase of optically active Tb^{3+} sites.

3.3. *Ce-doped oxygen-rich silicon oxides (Ce:ORSO)*

The Ce:ORSO samples have a constant Si content of 32 at.% and varying Ce contents of 0.01, 0.1, and 1.0 at.%, respectively. Figure 9 shows the PL spectra of the 1.0 at.% Ce sample as-deposited or after annealing at 800 and 1200°C, respectively. All spectra show an intense broad peak with a pronounced shoulder at longer wavelengths. The main peaks

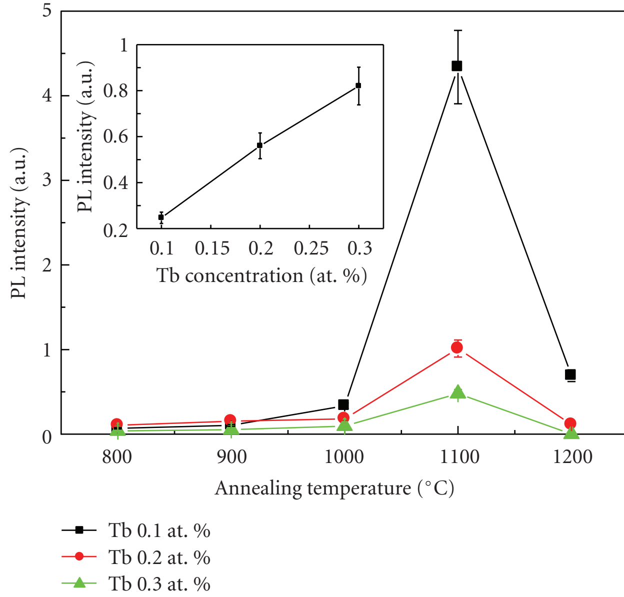

Figure 8: PL peak intensities of Si-ncs from the Tb:SRSO samples with various Tb concentrations as a function of annealing temperature. The inset shows the PL intensity of Tb^{3+} at 546 nm from Tb: SRSO samples after annealing at 1200°C as a function of Tb concentration.

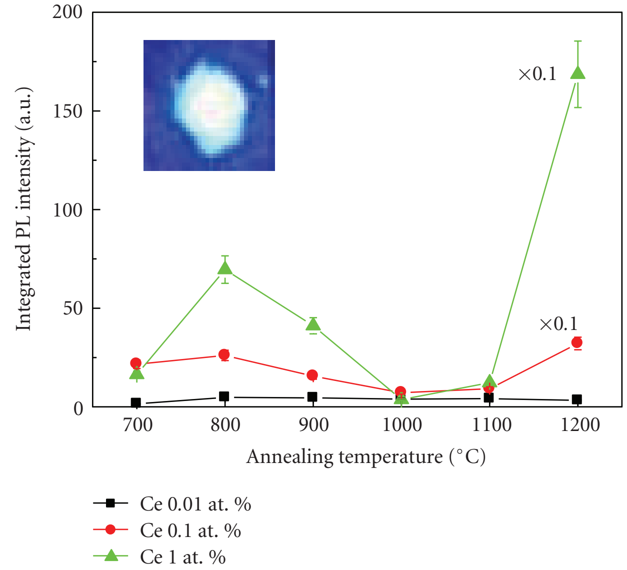

Figure 10: Integrated PL intensities in the range of 350–700 nm from the Ce:ORSO samples with various Ce concentrations as a function of annealing temperature. The inset shows an image of strong blue emission from the 1.0 at.% Ce sample after annealing at 1200°C taken by camera.

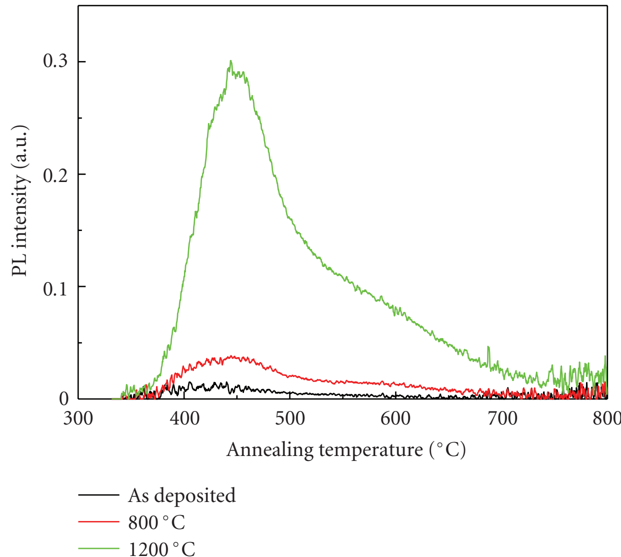

Figure 9: PL spectra of a Ce:ORSO sample containing 1.0 at.% Ce, as-deposited or after annealing at 800 and 1200°C, respectively.

were observed at 400, 422, and 460 nm from the samples as-deposited or annealed at 800 and 1200°C, respectively. The other two samples containing 0.01 and 0.1 at.% Ce have similar spectral shapes and peak positions.

Cerium can exist in both trivalent and tetravalent forms when embedded in the host materials by losing two 6s electrons and either one or two 4f electrons. Ce^{4+} is optically inactive due to the lack of 4f electrons. Although the 4f states are shielded by 5s and 5p states, the 5d states into which the 4f electron will be excited are exposed to the surrounding ligands. As previously discussed, the PL properties of Ce ions are highly dependent on the surrounding environment. Therefore, the changes in the spectral shapes, peak positions, and intensities strongly suggest the evolution of the film structure [13].

Unlike Tb, Ce^{3+} usually has a broad absorption band around 330 nm. The observed emissions originate from 5d-4f transitions of the Ce^{3+} in the films. Similar PL features have been observed from Ce doped SiO_2 prepared by the sol-gel method [34]. As the films were deposited under oxygen-rich conditions, most of the Ce ions exist as quadrivalent and possibly in the form of CeO_2. Since the Ce^{4+} ions are the dominant species in the as-deposited samples and only few optically active Ce^{3+} ions exist, the corresponding emission intensity is low.

Figure 10 shows the integrated normalized PL intensity in the range of 350–700 nm for the above three Ce:ORSO samples as a function of annealing temperature. At all of annealing temperatures—except for 700 and 1000°C—the PL intensity increases with increasing Ce concentration. And a similar dependence of the PL intensities on annealing temperatures was observed despite of the Ce concentrations. The PL intensities increase with annealing temperature up to 800°C and then decrease with annealing temperature up to 1000°C. At 1100°C, the intensities begin to increase again and reach the greatest value at 1200°C.

When annealed in an inert ambient at 700 and 800°C, the increase in emission intensities can be attributed to the increasing Ce^{3+}/Ce^{4+} ratio. Previous studies on CeO_2 have shown that at high temperatures, crystallized stoichiometric CeO_2 tends to form Ce_6O_{11} in order to lower the O/Ce

ratio through the migration of oxygen vacancies [35]. It appears that under these conditions, Ce^{3+} ions are more stable than Ce^{4+} ions. Furthermore, due to the concentration difference between the film and surrounding environment, some oxygen may be released from the film during the annealing process, which possibly leads to a local oxygen deficiency facilitating the deoxidization of Ce^{4+} ions.

It was reported that Ce^{3+} can form two types of optical centers depending on whether their surrounding environment was composed mainly of Ce^{4+} or Ce^{3+} ions. The former were observed to exhibit a shorter emission wavelength than the latter [36]. Our results are consistent with this finding, with a red shift of emission wavelength being observed for samples after annealing at 800°C or greater.

The decrease in emission intensity between anneals from 800 to 1000°C can be attributed to the clustering of Ce^{3+} ions leading to a quenching of the luminescence as this quenching is more profound in the samples with greater Ce concentrations. At these temperatures, the SiO_x matrix begins to form a more uniform and stable structure. Correspondingly, the number of nonbridging oxygen (NBO) defects is reduced significantly. As the temperature further increases, more Ce^{3+} ions form clusters to share the limited amount of NBO, and emissions from the Ce^{3+} ions are quenched by transferring their energy to other Ce^{3+} ions in the vicinity [37].

Several groups have observed similar UV/blue light emission from CeO_x/SiO_x or CeO_x/Si films annealed at 1000°C or greater in inert or reducing ambients [35, 38, 39]. However, the origin of the emission still remains controversial. Morshed et al. [35] observed the emission from CeO_2/Si films after rapid thermal annealing in Ar at 1000°C peaking at 400 nm. This emission was attributed to the formation of Ce_6O_{11} around the CeO_2/Si interface. Choi et al. [38] observed a weak 388 nm emission from a CeO_x/Si film and an intense 358 nm emission from (CeO_x + Si)/Si and (CeO_x + Si)/SiO_x/Si films after annealing in N_2 at 1100°C. Significant diffusion of Si from the substrate into CeO_2 and the formation of two cerium silicate phases, $Ce_2Si_2O_7$ and $Ce_{4.667}(SiO_4)_3O$, at the interface were observed. The 358 nm emission was attributed to $Ce_2Si_2O_7$ phase, and the weak 388 nm emission to the $Ce_{4.667}(SiO_4)_3O$ phase. Kępiński et al. [39] observed emission peaking at 400 nm from CeO_2/SiO_2 samples subjected to anneal in H_2 at 1050 and 1100°C and assigned it to an unidentified cerium silicate with some structural similarity to tetragonal $Ce_2Si_2O_7$ silicate. Therefore, in our study, the abrupt increase of the emission intensity at annealing temperatures greater than 1100°C may also suggest the formation of Ce silicate. At this high temperature, Ce^{3+} ions may acquire enough energy to interact with the surrounding Si and O atoms and reorganize to form a more stable structure.

A detailed study of the effects of high-temperature annealing on the structural evolution of these samples is in progress. Preliminary results from Fourier transform infrared spectroscopy show the emergence of new sharp absorption bands after the sample was annealed at 1200°C, similar to the peaks characteristic of $Ce_2Si_2O_7$ silicate, while there are still differences in both numbers and positions of absorption bands between them (data not shown).

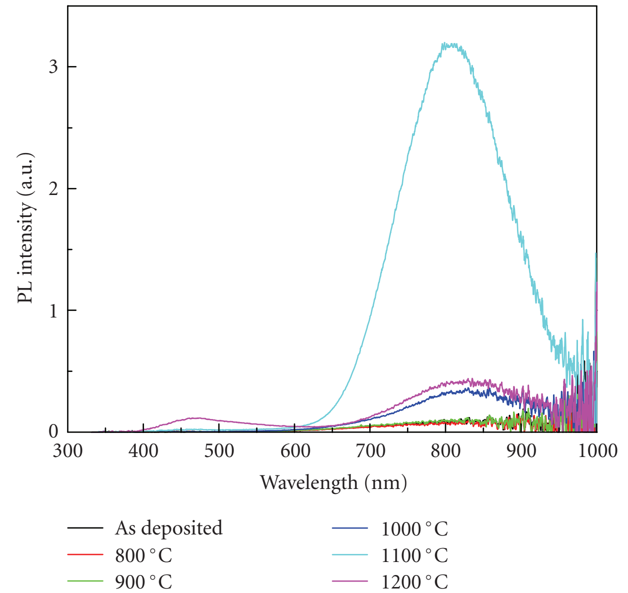

Figure 11: PL spectra of a Ce:SRSO sample containing 0.04 at.% Ce, as-deposited or annealed at various temperatures in the range of 800–1200°C.

The greatest intensity was observed from the 1.0 at.% Ce sample subjected to a 1200°C anneal which has the highest Ce concentration in the samples we studied. The inset of Figure 10 shows the emission picture taken by a camera. The Ce emission from this sample was 230 times greater than that of the as-deposited sample. In fact, after annealing at 800 or 1200°C, both the 0.1% Ce and 1.0% Ce samples exhibit such strong emissions that they can be easily observed under very bright room lighting condition. Considering that the excitation power is as low as 17 mW, the emission intensities are quite outstanding.

3.4. Ce-doped silicon-rich silicon oxide (Ce:SRSO)

The Ce:SRSO sample has Si and Ce content of 40 and 0.04 at.%, respectively. Figure 11 shows the PL spectra of the sample as deposited or annealed at various temperatures. There is no appreciable emission from the as-deposited sample. After annealing at 800°C, the sample shows a broad emission band centered at 800 nm, the emission intensity of which increases with annealing temperature until 1100°C. After annealed at 1200°C, the emission decreases by a factor of 8 and another weak broad emission band centered at 450 nm emerges.

It is evident that the 800 nm emission originates from the precipitated Si-ncs upon annealing. We attribute the 450 nm emission to the Ce^{3+} ions in the film. The enhancement of the Si-ncs emission intensity with annealing temperature indicates the formation of more Si-ncs in the same manner as was observed in Tb:SRSO samples. The absence of Ce emission at annealing temperatures lower than 1200°C is also

possibly due to the competition between Si-ncs and Ce ions in the absorption of excitation photons.

4. CONCLUSIONS

Rare-earth (Tb or Ce) doped silicon oxides (silicon-rich or oxygen-rich) were deposited by ECR-PECVD. The successful in situ incorporation of high concentrations of optically active rare-earth ions was demonstrated. The dependence of the PL properties on Si/O ratio, doping concentration, and annealing temperature was investigated.

Green Tb emission was observed in both oxygen-rich and silicon-rich samples. The excitation wavelength is not resonant with any optical absorption band of Tb^{3+}. We propose that in oxygen-rich films, the organic ligands introduced from the deposition process may serve as the sensitizers to excite Tb emission while Si-ncs serve as the sensitizers in silicon-rich films.

Violet/blue Ce emission was observed in both oxygen-rich and silicon-rich films. An abrupt increase of Ce emission intensity in oxygen-rich films after annealing at 1200°C is possibly due to the formation of Ce silicate. In silicon-rich films, the Ce emission was absent at annealing temperatures lower than 1200°C.

It was found that by choosing appropriate compositions and annealing temperatures, the Ce and Tb PL intensities can be enhanced significantly. The highest Ce PL intensity was observed from the sample containing 32 at.% Si and 1.0 at.% Ce annealed at 1200°C which has the highest Ce concentration in the samples we examined. The highest Tb PL intensity was observed from the sample containing 32 at.% Si and 0.4 at.% Tb annealed at 800°C. Those emissions were very bright and can be easily observed under room lighting condition.

ACKNOWLEDGMENTS

The authors would like to acknowledge Dr. W. Lennard and J. Hendriks, both at the University of Western Ontario, for their expert help in RBS measurements, J. Garrett and G. Pearson at McMaster University for technical support in annealing, and J. Huang and F. Pearson at McMaster University for TEM analysis. We thank H. (Charlie) Zhang for many hours of film depositions. This work has been cofunded by the Ontario Photonics Consortium (OPC), Ontario Centres of Excellence (OCE), Centre for Photonics Fabrication Research (CPFR), and Canadian Institute for Photonic Innovation (CIPI). We are grateful for financial and technical support from Group IV Semiconductor Inc. (Kanata, Ontario) and Johnsen-Ultravac (Burlington, Ontario).

REFERENCES

[1] G. T. Reed and A. P. Knights, *Silicon Photonics: An Introduction*, John Wiley & Sons, New York, NY, USA, 2004.

[2] D. J. Lockwood, *Light Emission in Silicon: From Physics to Devices*, Academic Press, New York, NY, USA, 1998.

[3] A. Liu and M. Paniccia, "Advances in silicon photonic devices for silicon-based optoelectronic applications," *Physica E*, vol. 35, no. 2, pp. 223–228, 2006.

[4] S. Ossicini, L. Pavesi, and F. Priolo, *Light Emitting Silicon for Microphotonics*, Springer, Berlin, Germany, 2003.

[5] P. G. Kik and A. Polman, "Erbium-doped optical-waveguide amplifiers on silicon," *MRS Bulletin*, vol. 23, no. 4, pp. 48–54, 1998.

[6] A. J. Kenyon, "Recent developments in rare-earth doped materials for optoelectronics," *Progress in Quantum Electronics*, vol. 26, no. 4-5, pp. 225–284, 2002.

[7] G. H. Dieke, *Spectra and Energy Levels of Rare-Earth Ions in Crystals*, John Wiley & Sons, New York, NY, USA, 1968.

[8] A. Yoshida, Y. Nakanishi, and A. Wakahara, "Light emission from rare-earth-implanted GaN expected for full-color display," in *Smart Materials, Structures, and Systems*, vol. 5062 of *Proceedings of SPIE*, pp. 18–19, San Diego, Calif, USA, October 2003.

[9] N. D. Vieira Jr., I. M. Ranieri, L. V. G. Tarelho, et al., "Laser development of rare-earth doped crystals," *Journal of Alloys and Compounds*, vol. 344, no. 1-2, pp. 231–239, 2002.

[10] J. K. Sahu, Y. Jeong, D. J. Richardson, and J. Nilsson, "A 103 W erbium-ytterbium co-doped large-core fiber laser," *Optics Communications*, vol. 227, no. 1–3, pp. 159–163, 2003.

[11] B. V. Shul'gin, V. L. Petrov, V. A. Pustovarov, et al., "Scintillation neutron detectors based on ^{6}Li-silica glass doped with cerium," *Physics of the Solid State*, vol. 47, no. 8, pp. 1412–1415, 2005.

[12] L. Galambos, S. S. Orlov, L. Hesselink, Y. Furukawa, K. Kitamura, and S. Takekawa, "Doubly doped stoichiometric and congruent lithium niobate for holographic data storage," *Journal of Crystal Growth*, vol. 229, no. 1–4, pp. 228–232, 2001.

[13] M. Gaft, R. Reisfel, and G. Panczer, *Morden Luminescence Spectroscopy of Minerals and Materials*, Springer, Berlin, Germany, 2005.

[14] A. Polman and F. C. J. M. van Veggel, "Broadband sensitizers for erbium-doped planar optical amplifiers: review," *Journal of the Optical Society of America B*, vol. 21, no. 5, pp. 871–892, 2004.

[15] M. V. Wolkin, J. Jorne, P. M. Fauchet, G. Allan, and C. Delerue, "Electronic states and luminescence in porous silicon quantum dots: the role of oxygen," *Physical Review Letters*, vol. 82, no. 1, pp. 197–200, 1999.

[16] A. J. Kenyon, "Erbium in silicon," *Semiconductor Science and Technology*, vol. 20, no. 12, pp. R65–R84, 2005.

[17] A. J. Kenyon, M. Wojdak, I. Ahmad, W. H. Loh, and C. J. Oton, "Generalized rate-equation analysis of excitation exchange between silicon nanoclusters and erbium ions," *Physical Review B*, vol. 77, no. 3, Article ID 035318, 9 pages, 2008.

[18] A. J. Kenyon, P. F. Trwoga, C. W. Pitt, and G. Rehm, "The origin of photoluminescence from thin films of silicon-rich silica," *Journal of Applied Physics*, vol. 79, no. 12, pp. 9291–9300, 1996.

[19] J. Lee, J. H. Shin, and N. Park, "Optical gain at 1.5 μm in nanocrystal Si-sensitized Er-doped silica waveguide using top-pumping 470 nm LEDs," *Journal of Lightwave Technology*, vol. 23, no. 1, pp. 19–25, 2005.

[20] S.-Y. Seo and J. H. Shin, "Enhancement of the green, visible Tb^{3+} luminescence from Tb-doped silicon-rich silicon oxide by C co-doping," *Applied Physics Letters*, vol. 84, no. 22, pp. 4379–4381, 2004.

[21] A. Vedda, N. Chiodini, D. Di Martino, et al., "Rare-earth aggregates in sol-gel silica and their influence on optical properties," *Physica Status Solidi C*, vol. 2, no. 1, pp. 620–623, 2005.

[22] M. Flynn, J. Wojcik, S. Gujrathi, E. Irving, and P. Mascher, "The impact of deposition parameters on the optical and compositional properties of Er doped SRSO thin films deposited by ECR-PECVD," in *Proceedings of the Materials Research Society Symposium*, vol. 866, pp. 163–167, San Francisco, Calif, USA, March 2005.

[23] D. E. Blakie, O. H. Y. Zalloum, J. Wojcik, E. J. Irving, A. P. Knights, and P. Mascher, "Coupled luminescence centres in erbium-doped silicon rich silicon oxide thin films," in *Photonics North*, vol. 6343 of *Proceedings of SPIE*, p. 11 pages, Quebec City, Canada, June 2006.

[24] C. L. Heng, O. H. Y. Zalloum, T. Roschuk, D. Blakie, J. Wojcik, and P. Mascher, "Photoluminescence study of an Er-doped Si-rich siO_x film," *Electrochemical and Solid-State Letters*, vol. 10, no. 7, pp. K20–K23, 2007.

[25] O. H. Y. Zalloum, M. Flynn, T. Roschuk, J. Wojcik, E. Irving, and P. Mascher, "Laser photoluminescence spectrometer based on charge-coupled device detection for silicon-based photonics," *Review of Scientific Instruments*, vol. 77, no. 2, Article ID 023907, 8 pages, 2006.

[26] S. P. Depinna and D. J. Dunstan, "Frequency-resolved spectroscopy and its application to the analysis of recombination in semiconductors," *Philosophical Magazine B*, vol. 50, no. 5, pp. 579–597, 1984.

[27] M. Gaft, R. Reisfeld, and G. Pancezer, *Luminescence Spectroscopy of Minerals and Materials*, Springer, New York, NY, USA, 2005.

[28] M. Yoshihara, A. Sekiya, T. Morita, et al., "Rare-earth-doped SiO_2 films prepared by plasma-enhanced chemical vapour deposition," *Journal of Physics D*, vol. 30, no. 13, pp. 1908–1912, 1997.

[29] H. Amekura, A. Eckau, R. Carius, and Ch. Buchal, "Visible photoluminescence from Tb^{3+} ions implanted into a SiO_2 film on Si at room temperature," in *Proceedings of the International Conference on Ion Implantation Technology (IIT '99)*, vol. 2, pp. 925–928, Kyoto, Japan, June 1999.

[30] A. Polman, D. C. Jacobson, A. Lidgard, J. M. Poate, and G. W. Arnold, "Photoluminescence and structural characterization of MeV erbium-implanted silica glass," *Nuclear Instruments and Methods in Physics Research B*, vol. 59-60, part 2, pp. 1313–1316, 1991.

[31] H. Jeong, S.-Y. Seo, and J. H. Shin, "Excitation mechanism of visible, Tb^{3+} photoluminescence from Tb-doped silicon oxynitride," *Applied Physics Letters*, vol. 88, no. 16, Article ID 161910, 3 pages, 2006.

[32] B. Stannowski, J. K. Rath, and R. E. I. Schropp, "Growth process and properties of silicon nitride deposited by hot-wire chemical vapor deposition," *Journal of Applied Physics*, vol. 93, no. 5, pp. 2618–2625, 2003.

[33] H. Ofuchi, Y. Imaizumi, H. Sugawara, H. Fujioka, M. Oshima, and Y. Takeda, "Fluorescence XAFS study on local structures around Tb ions implanted in SiO_2 on Si," *Nuclear Instruments and Methods in Physics Research B*, vol. 199, pp. 231–234, 2003.

[34] G. Q. Xu, Z. X. Zheng, W. M. Tang, and Y. C. Wu, "Luminescence property of Ce^{3+}-doped silica decorated with S^{2-} and Cl^- anions," *Journal of Luminescence*, vol. 126, no. 2, pp. 475–480, 2007.

[35] A. H. Morshed, M. E. Moussa, S. M. Bedair, R. Leonard, S. X. Liu, and N. El-Masry, "Violet/blue emission from epitaxial cerium oxide films on silicon substrates," *Applied Physics Letters*, vol. 70, no. 13, pp. 1647–1649, 1997.

[36] G. E. Malashkevich, E. N. Poddenezhny, I. M. Melnichenko, and A. A. Boiko, "Optical centers of cerium in silica glasses obtained by the sol-gel process," *Journal of Non-Crystalline Solids*, vol. 188, no. 1-2, pp. 107–117, 1995.

[37] H. Bi, W. Cai, H. Shi, B. Yao, and L. Zhang, "Effects of annealing and Al co-doping on the photoluminescence of Ce^{3+}-doped silica prepared by a sol-gel process," *Journal of Physics D*, vol. 33, no. 19, pp. 2369–2372, 2000.

[38] W. C. Choi, H. N. Lee, Y. Kim, H. M. Park, and E. K. Kim, "Luminescence from the thermally treated cerium oxide on silicon," *Japanese Journal of Applied Physics*, vol. 38, no. 11, pp. 6392–6393, 1999.

[39] L. Kępiński, M. Wołcyrz, and M. Marchewka, "Structure evolution of nanocrystalline CeO_2 supported on silica: effect of temperature and atmosphere," *Journal of Solid State Chemistry*, vol. 168, no. 1, pp. 110–118, 2002.